Supporting Information

Iron-Coordinating π-Conjugated Semiconducting Polymer: Morphology and Charge Transport in Organic Field-Effect Transistors

P. Blake J. St. Onge,[a,‡] Tzu-Chien Chen,[b,‡] Adam Langlois,[a] Aneeta Younus,[a] I Jo Hai,[b] Bi-Hsuan Lin,[c] Yu-Cheng-Chiu,[b,d],* and Simon Rondeau-Gagné [a,*]

[a] Department of Chemistry and Biochemistry, Advanced Materials Centre of Research (AMCORe), University of Windsor, 401 Sunset Ave., Windsor, Ontario, Canada, N9B 3P4

[b] Department of Chemical Engineering, National Taiwan University of Science and Technology, Taipei 106, Taiwan

[c] National Synchrotron Radiation Research Center, Hsinchu 30076, Taiwan

[d] Advanced Research Center for Green Materials Science and Technology, National Taiwan University, Taipei 10617, Taiwan.

[‡] These authors have equally contributed to this work.

Table of Contents

General Procedure and Materials

Materials. Commercial reactants were used without further purification unless stated otherwise. All the solvents used in these reactions were distilled prior to use. Tetrakis(triphenylphosphine)palladium was purchased from Sigma Aldrich. (E)-1,2-bis(5-(trimethylstannyl)thiophen-2-yl)ethene (TVT), diketopyrrolopyrrole, and compounds **1, 2** and **5** were synthesized according to literature.[1-6]

Instrumentation. NMR Spectra were recorded at room temperature in CDCl$_3$, CD$_3$CN and d-DMSO solutions with a Bruker 300 MHz spectrometer. Chemical shifts are reported in ppm, relative to external standards. Cyclic voltammograms were taken in a 0.1M solution of TBAPF$_6$ in anhydrous acetonitrile at room temperature. Pt was used as working electrode and counter electrode. Ag|AgCl was used as non-aqueous reference. The scan rate of measurements was 100 mV/s. The surface structure of the polymer film was obtained using a Multimode atomic force microscope (AFM, Digital Instruments) operated in the tapping mode at room temperature. Images were collected using the Nanoscope 6 software and processed using the WSxM 5.0 Develop 8.0 software. The surface mechanical properties (elastic moduli) were characterized using PeakForce™ in tapping mode (Dimension Icon, Bruker). Number average molecular weight (Mn), weight average molecular weight (Mw), and polydispersity index (PDI) were evaluated by high temperature size exclusion chromatography (SEC) using 1,2,4-trichlorobenzene and performed on a EcoSEC HLC-8321GPC/HT (Tosoh Bioscience) equipped with a single TSKgel GPC column (GMHHR-H; 300 mm × 7.8 mm) calibrated with monodisperse polystyrene standards. The samples were prepared using 1 mg/mL of sample in trichlorobenzene (TCB), which were allowed to stir at 80 ^{0}C for 12 h prior to injection. The analysis of the samples was performed at 180 ^{0}C with a flow rate of 1.0 mL/min with injection quantities of 300 μL. The data was collected and

integrated using EcoSEC 8321GPC HT software suite. The samples were analyzed by X-ray photoelectron spectroscopy (XPS) using a Kartos AXIS Supra X-Ray photoelectron spectrometer. XPS can detect all elements except hydrogen and helium and probes the surface of the sample to a depth of 7-10 nanometers which has detection limits ranging from 0.1 to 0.5 atomic percent. XPS survey spectra were obtained from an area of approximately 300 x 700 μm using a pass energy of 160 eV. XPS High resolution spectra were obtained from an area of approximately 200 x 700 μm using a pass energy of 20 eV. High resolution spectra are charge corrected to the main line of the C 1s to 285.0 eV. The relative degree of crystallinity for polymer films were performed by GIXRD on beamline BL13A with a wavelength of 1.02042Å (12kev) at the Taiwan Light Source (TLS) of National Synchrotron Radiation Research Center (NSRRC). All two-dimensional images of GIXRD were collected in reflection mode by Charge coupled device (MAR165 CCD) X-ray detector. Elements in solid film were analyzed by energy-dispersive (4 ~ 15keV). X-ray Fluorescence (XRF) and X-Ray near edge absorption spectroscopy (XANES) were performed at the X-ray nanoprobe beamline, TPS 23A, at the Taiwan Photon Source (TPS) of the National Synchrotron Radiation Research Center (NSRRC) in Taiwan. A silicon drift detector (SDD; Vortex-ME4, HITACHI) was utilized for XRF data collection. The essential advantage for TPS23A is using the Montel optics forming a nanometer-focal spot (focused spot size: 40 nm) from two sequential reflections by two identical mirrors nesting side-by-side. Absorbance and fluorescence titration experiments were performed by preparing solutions of known concentration of the fluorophore and quencher. Subsequent solutions were prepared from these solutions such that the concentration of the fluorophore remained constant while the concentration of the quencher was varied. The error in concertation was calculated based on the error from the initial weight of the samples and the error associated with the volumetric glassware used to prepare the

solutions. Absorption spectra were recorded on an Agilent Technologies 8453 Diode Array UV-Vis spectrometer, with a spectral resolution of 1 nm in a 1 cm quartz cuvette. The error on the measurement was obtained from the standard deviation provided by the instrument. Each absorption measurement was averaged over three measurements. Emission spectra were recorded on QM-400 phosphorimeter by PTI using a 477 nm excitation from a xenon lamp. The spectra were averaged over three scans and the standard deviation in intensity was used as the error in the measured value. Fluorescence lifetime measurements were performed by TCSPC on a FLS-980 phosphorimeter from Edinburgh Instruments using a 477 nm ps-laser source from Delta Diode operating at a repetition rate of 8 MHz. The Fluorescence decays were fit using distribution analysis.

Sample preparation. The complexation of the DPP pincer monomer was performed by adding a selected amount of $Fe(BF_4)_2$ to monomer **4** in solution. **P(DPPTVT-MeBZIMPY)-Fe** was prepared by adding a selected quantity $Fe(BF_4)_2$ (1.5 equivalents per metal-coordinating DPP moiety) to a solution of P(DPPTVT-MeBZIMPY). The solution was stirred overnight and filtered on 0.45 μm filter to remove any potential aggregates, and directly used for further characterization.

Grazing Incident X-Ray Diffraction (GIXRD). To get accurate comparison on crystallinity, the relative degree of crystallinity (rdoc) was calculated for P(DPPTVT-MeBZIMPY) after thermal annealing at 200°C, before and after metal coordination. Defined by the ratio of intensity of two diffraction peaks in thin films, the rdoc was calculated from the pole figures for the (200) diffraction peak determined from the GIXRD patterns by integrating the area under each curve separately to get an integrated intensity. To get an accurate comparison, the rdoc for P(DPPTVT-MeBZIMPY) without metal has been fixed to 1. Based on this calculation, the integrated intensities

of P(DPPTVT-MeBZIMPY) and P(DPPTVT-MeBZIMPY)-Fe have been calculated to 4008808 and 397775, respectively. The rdoc of P(DPPTVT-MeBZIMPY)-Fe, in comparison to P(DPPTVT-MeBZIMPY), was determined to be 0.992.

Device Fabrication. FET devices were fabricated on highly doped n-type Si(100) wafer with a 300 nm thick SiO_2 functionalized with an n-octadecyltrimethoxysilane (OTS) self-assembled monolayer, according to the reported method. The OTS-treated substrate was washed with toluene, acetone and isopropyl alcohol, and then dried with nitrogen before use. The organic semiconductor thin films were spin-cast on the OTS-treated substrates and controlled the thickness at ~40-50 nm from prepared polymer solutions in chlorobenzene (4 mg mL−1). The thermal annealing process was carried out inside a N_2-filled glove box. A top-contact gold electrode (50 nm) was subsequently deposited by evaporation through a shadow mask with a channel length (L) and width (W) defined as 50 and 1000 μm, respectively. All the measurements of the transistor memories were conducted using a Keithley 4200-SCS semiconductor parameter analyzer (Keithley Instruments Inc., Cleveland, OH, USA) in an N2- filled glove box at room temperature.

Experimental Procedure
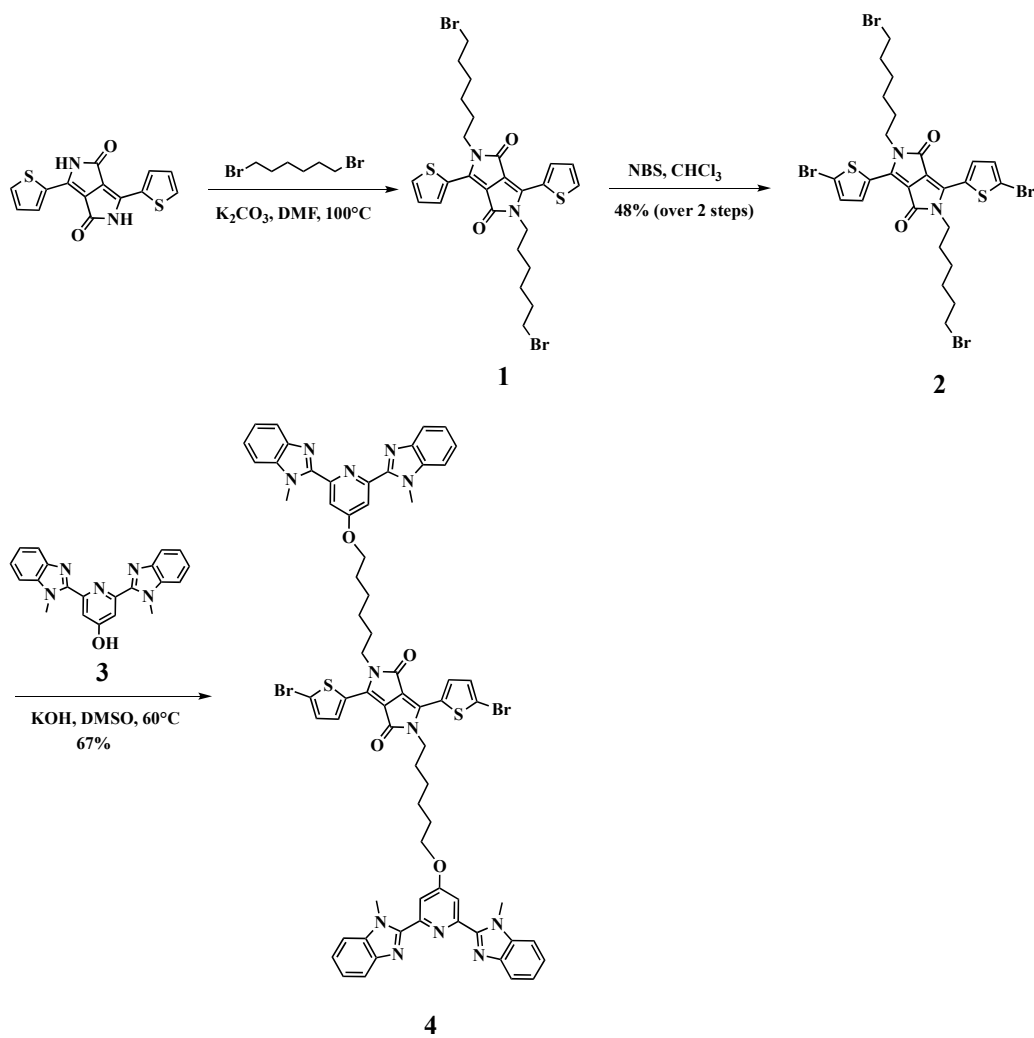
Scheme S1. *Synthetic pathway towards DPP-MeBZIMPY monomer (compound **4**) for metal-complexation and polymerization.*
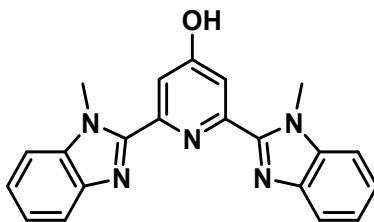
2,6-Bis(1'-methylbenzimidazolyl)-4-hydroxypyridine. The compound was synthesized according to previous reported literature with slight modifications.[7] To a purged flame dried 250 mL round-bottom flask, n-methyl-1,2-phenylenediamine (2.05 g, 16.8 mmol) and chelidamic acid (1.49 g, 8.21 mmol) was added to polyphosphoric acid (20 mL). The reaction mixture was then heated to 220 ^{0}C and allowed to stir for 12 hours. While hot, the reaction mixture was poured into ice cold deionized water to produce a dark blue precipitate. The precipitate was then filtered and collected, which was then resuspended in deionized water at 70 ^{0}C. Small amounts of sodium carbonate were added to the solution to adjust the pH to 7. The reaction mixture was then filtered and dried to produce compound **3** as a light grey powder. Yield: 2.60 g (89 %). ^{1}H NMR (d$_6$-DMSO) δ: 7.98 (s, 2H), 7.82 (s, 2H), 7.32 (m, 6H), 4.10 (s, 6H). ^{13}C NMR (d$_6$-DMSO) δ: 165.2, 150.9, 141.85, 137.0, 122.4, 119.4, 110.8, 32.5.
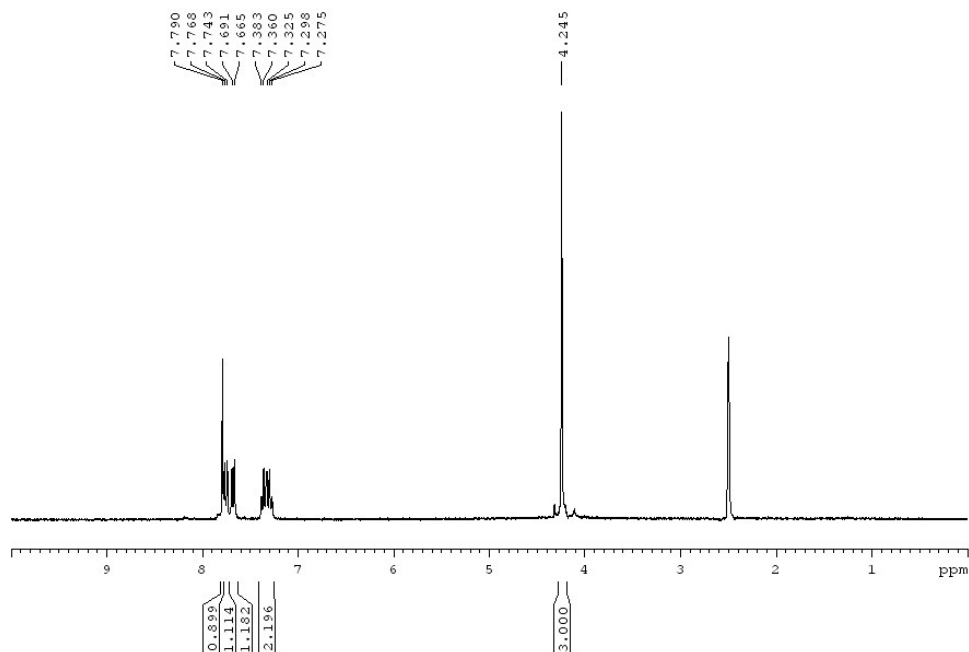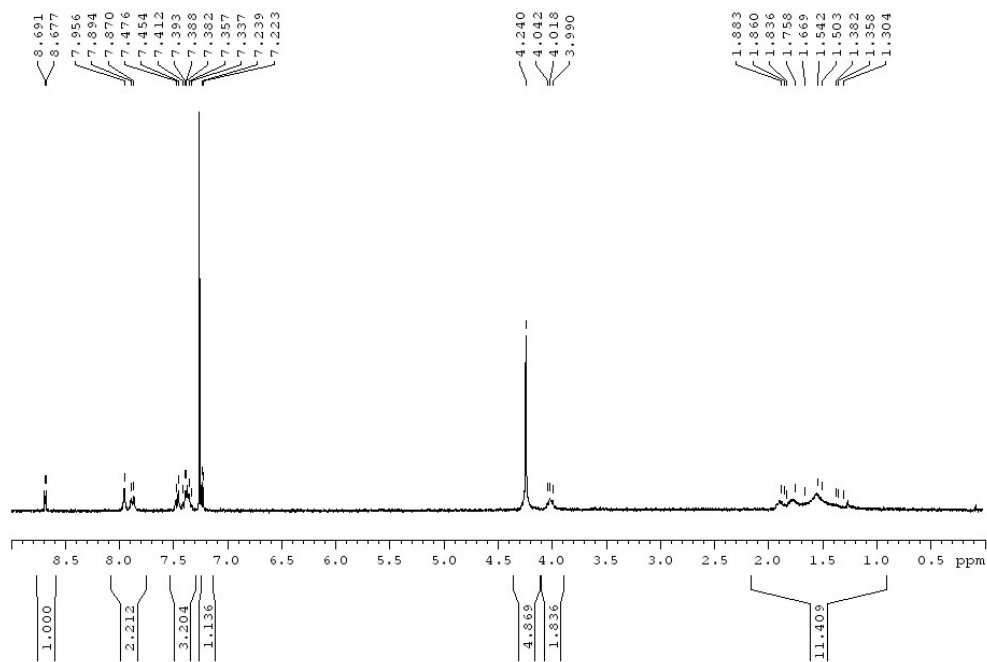

^{1}H NMR of Compound **3**.
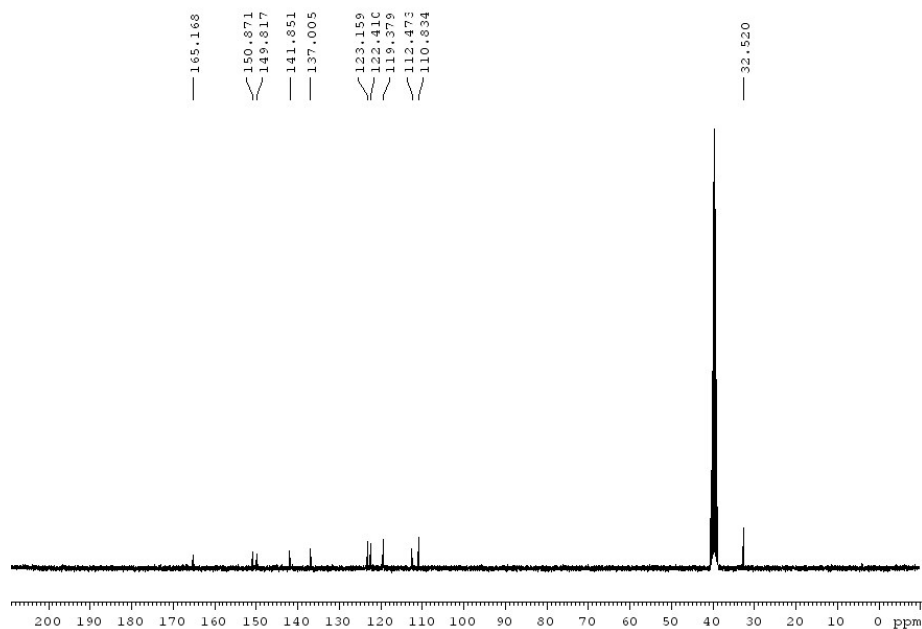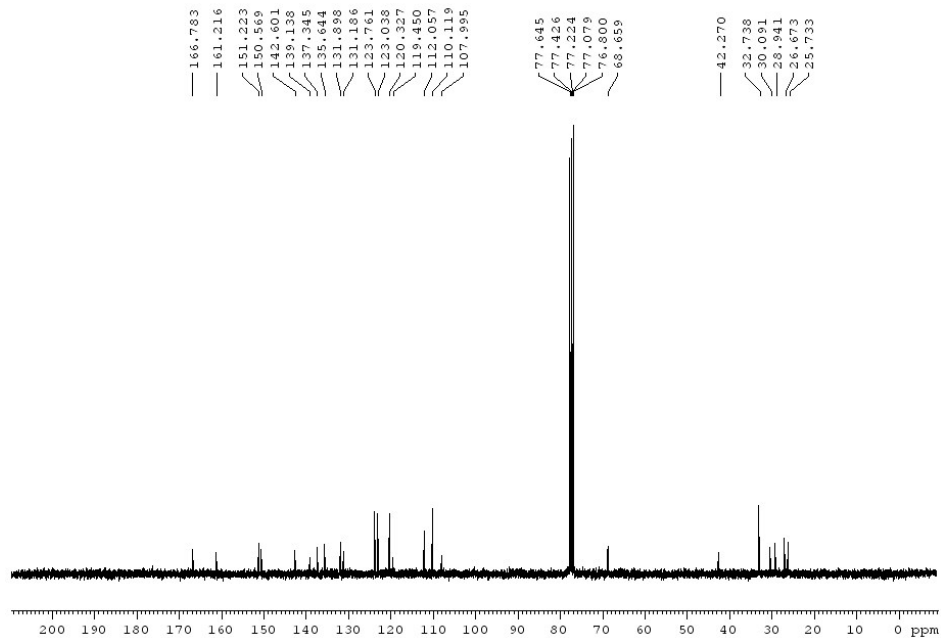
^{13}C NMR of Compound **3**.
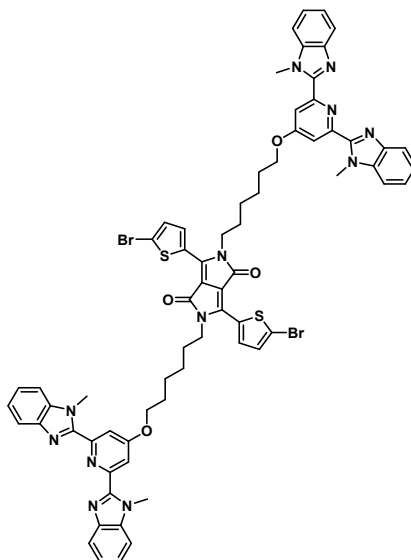
2,5-bis(6-((2,6-bis(1-methyl-1H-benzo[d]imidazol-2-yl)pyridin-4-yl)oxy)hexyl)-3,6-bis(5-bromothiophen-2-yl)-2,5-dihydropyrrolo[3,4-c]pyrrole-1,4-dione. To a purged flame dried flask, K_2CO_3 (447 mg, 3 mmol) was added to DMF (40 mL). Nitrogen was then bubbled through the

solution for 30 min while stirring. To the solution OH-MeBZIMPY (232 mg, 653 μmol) is added, followed by the addition of 2,5-bis(6-bromohexyl)-3,6-bis(5-bromothiophen-2-yl)-2,5-dihydropyrrolo[3,4-c]pyrrolo-1,4-dione (250 mg, 317 μmol). The solution is then refluxed for 36 hours. The dark purple solution is then extracted with $CHCl_3$ and H_2O, dried with Na_2SO_4 and reduced under pressure. The dark purple product is then precipitated out in hexane to obtain a dark purple solid. Flash column chromatography is then performed in pure $CHCl_3$, then acetone to where the collected solution is reduced under pressure to obtain compound **4** as a bright purple powder. Yield: 280 mg (67 %). ^{1}H NMR ($CDCl_3$) δ: 8.68 (d, 1H, J = 4 Hz), 7.96-7.87 (m, 2H), 7.47-7.36 (m, 3H), 7.23 (d, 2H, J = 4 Hz), 4.24 (s, 5H), 4.02 (m, 2H), 1.88-1.30 (m, 12H). ^{13}C NMR ($CDCl_3$) δ: 166.7, 161.2, 151.2, 150.6, 142.6, 139.1, 135.7, 131.9, 131.2, 123.8, 123.0, 120.3, 119.5, 112.0, 110.1, 108.0, 68.7, 42.7, 32.7, 30.1, 28.9, 26.67, 25.7. HRMS (ESI-ToF) calcd for $[M+Na]^+$: 1353.2561, found 1353.2577.
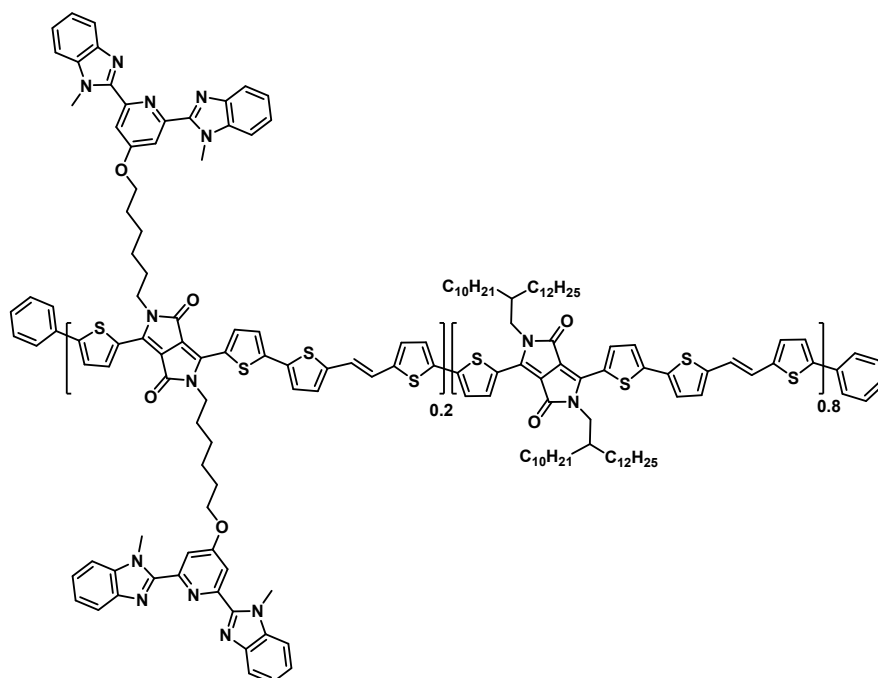

^{1}H NMR of **4** in $CDCl_3$.

^{13}C NMR of **4** in CDCl$_3$
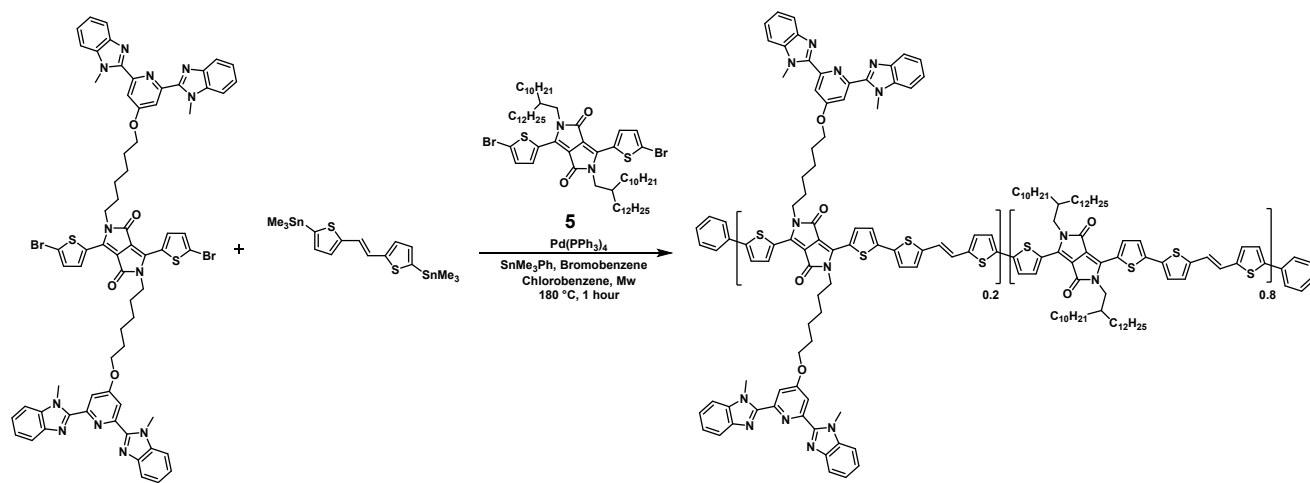
Scheme S2. *Synthesis of P(DPPTVT-MeBZIMPY).*

P(DPPTVT-MeBZIMPY). To a microwave vessel, compound **4** (34.75 mg, 0.03 mmol), compound **5** (78.65 mg, 0.06 mmol) and $(SnMe_3)_2$TVT (45 mg, 0.09 mmol) were added. Chlorobenzene (3.4 mL) was charged to the microwave vessel and the solution was degassed for 40 minutes. $Pd(PPh_3)_4$ (2.00 mg, 0.001 mmol) were added to the microwave vessel. The polymerization reaction was carried out using the microwave at 300W, 180 ^{0}C for 1 hour. The reaction mixture became dark green in color. $SnMe_3$Ph (0.01 mL, 0.08 mmol) was added to the vessel and was reacted again for 7 minutes at 300W, 160 ^{0}C. Final end-capping was carried out using the microwave, to where bromobenzene (0.01 mL, 0.08 mmol) was added to the microwave vessel utilizing the same conditions listed at 160 ^{0}C. Upon polymerization, the materials were precipitated in methanol and purified by Soxhlet extraction successively in methanol, acetone, and hexanes. The materials were collected with chlorobenzene, precipitated in methanol and dried under vacuum. HT-GPC was performed on the material which yielded a M_n, M_w, and PDI of 10.9 kDa, 17.6 kDa and 1.76 respectively.
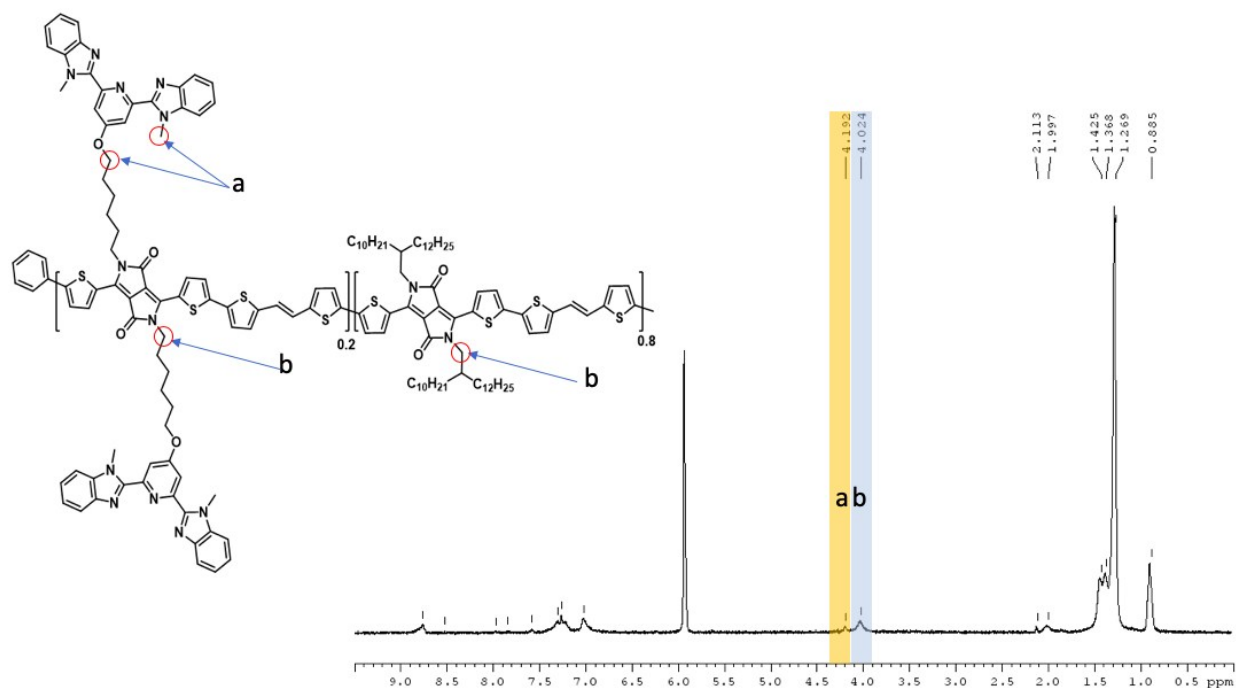
Materials and Devices Characterization

Figure S1. *Composition of P(DPPTVT-MeBZIMPY) as determined by ^1H NMR in 1,1,2,2-tetrachloroethane-d_2 at 120 ^oC. Experimental calculation of polymer ratios were determined from examining H_a and H_b assuming 10 repeat units.*
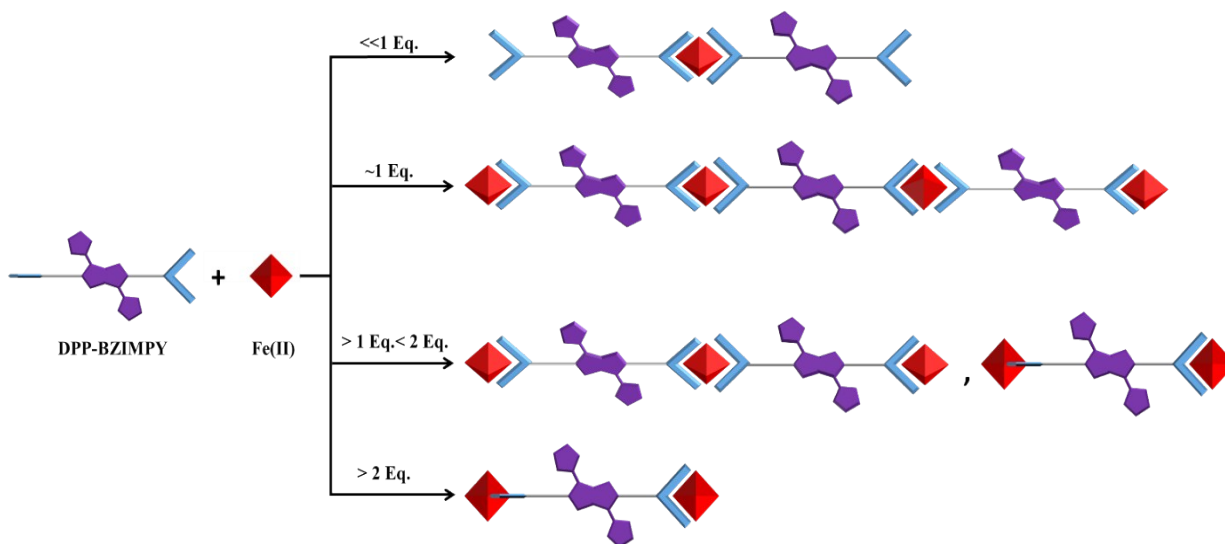

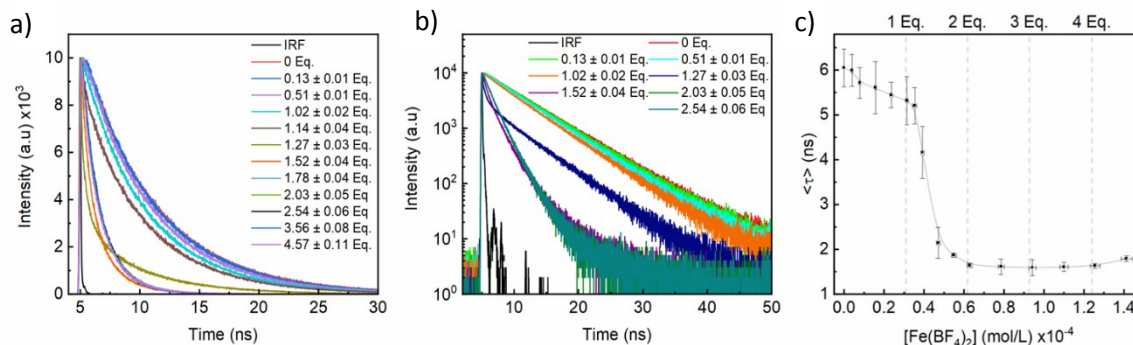**Figure S2.** *Product formation as a function of Fe(BF$_4$)$_2$ concentration.*

Figure S3. *Fluorescence lifetime titration experiment: Measured fluorescence decays as a function of number of added equivalents of Fe(BF$_4$)$_2$ A) in a linear scale, B) in a log scale and C) the average fluorescence lifetime as a function of Fe(BF$_4$)$_2$ concentration.*
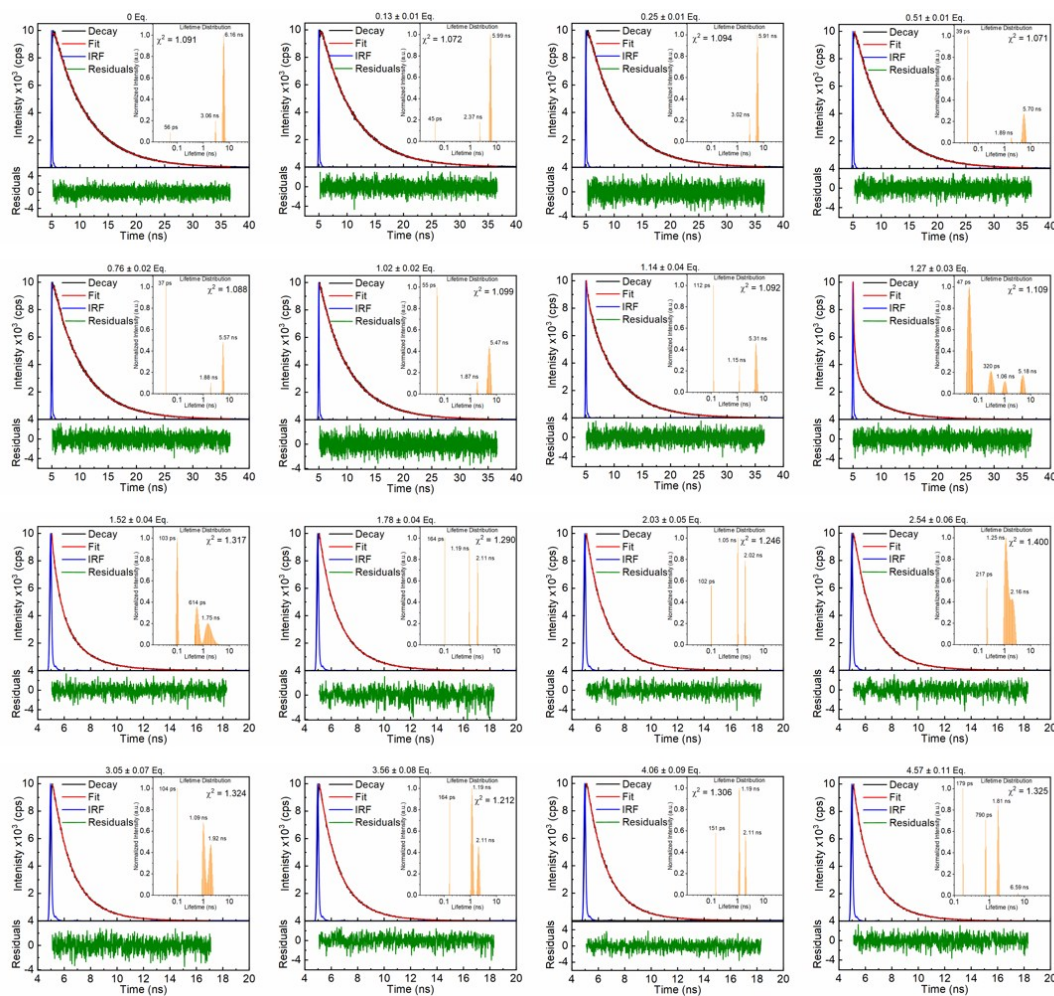

Figure S4. *Fluorescence titration experiment: Excited state lifetime decay traces and fits as a function of Fe(BF$_4$)$_2$ concentration*

Table S1. *Fluorescence titration results*

[Fe(BF$_4$)$_2$] (mol/L) x 10^{-5}	Eq. Fe(BF$_4$)$_2$	I (a.u)[a]	I$_0$/I	$\langle\tau\rangle$ (ns)[b]	$\langle\tau_0\rangle$/$\langle\tau\rangle$
0	0	39.168 ± 0.004	1.000 ± 0.001	6.049 ± 0.423	1.00 ± 0.10
0.393 ± 0.040	0.13 ± 0.01	29.7 ± 0.2	1.32 ± 0.01	5.991 ± 0.353	1.01 ± 0.09
0.785 ± 0.042	0.25 ± 0.01	21.7 ± 0.1	1.803 ± 0.009	5.714 ± 0.346	1.05 ± 0.10
1.57 ± 0.03	0.51 ± 0.01	13.5 ± 0.2	2.90 ± 0.03	5.606 ± 0.583	1.08 ± 0.14
2.36 ± 0.07	0.76 ± 0.02	5.34 ± 0.02	7.33 ± 0.02	5.441 ± 0.285	1.11 ± 0.10
3.14 ±0.06	1.02 ± 0.02	2.58 ± 0.05	15.19 ± 0.27	5.318 ± 0.538	1.14 ± 0.14
3.53 ±0.01	1.14 ± 0.04	1.06 ± 0.03	36.89 ± 1.05	5.204 ± 0.405	1.16 ± 0.12
3.93 ± 0.09	1.27 ± 0.03	0.29 ± 0.04	135.8 ± 18.0	4.159 ± 0.578	1.45 ± 0.23
4.71 ± 0.09	1.52 ± 0.04	0.343 ± 0.009	114.1 ± 3.2	2.143 ± 0.347	2.82 ± 0.50
5.50 ± 0.01	1.78 ± 0.04	0.62 ± 0.02	63.66 ± 2.32	1.867 ± 0.045	3.24 ± 0.24
6.28 ±0.01	2.03 ± 0.05	0.771 ± 0.008	50.83 ± 0.55	1.642 ± 0.050	3.68 ± 0.28
7.85 ±0.02	2.54 ± 0.06	0.98 ± 0.03	40.09 ± 1.29	1.611 ± 0.171	3.75 ± 0.48
9.42 ± 0.02	3.05 ± 0.07	1.14 ± 0.04	34.25 ± 1.25	1.589 ± 0.184	3.81 ± 0.51
10.99 ± 0.02	3.56 ± 0.08	1.28 ± 0.01	30.52 ± 0.29	1.605 ± 0.100	3.77 ± 0.35
12.56 ± 0.02	4.06 ± 0.09	1.335 ± 0.007	29.31 ± 0.16	1.631 ± 0.052	3.71 ± 0.29
14.13 ± 0.03	4.57 ± 0.11	1.28 ± 0.02	30.57 ± 0.51	1.788 ± 0.060	3.38 ± 0.26

a. Average emission intensity on three scans excited at 477 nm

$$<\tau>=\frac{\sum\limits_{i=1}^{n}B_i\tau_i^2}{\sum\limits_{i=1}^{n}B_i\tau_i}$$

b. Average emission lifetime calculated using the equation where B_i is the pre-exponential factor(s) and τ is the lifetime(s) obtained from a distribution analysis fit. The error on $\langle\tau\rangle$ is the propagation of the standard deviation for each lifetime component.

Table S2. *Fluoresce lifetimes upon addition of Fe(BF₄)₂*

Eq. Fe(BF$_4$)$_2$	τ (ns)[a]	Eq. Fe(BF$_4$)$_2$	τ (ns)[a]
0	0.056 ± 0.0007 (0.02 %) 3.016 ± 0.093 (3.60 %) 6.164 ± 0.431 (96.38 %) χ^2=1.091	1.52 ± 0.04	0.103 ± 0.007 (5.27 %) 0.614 ± 0.083 (21.73 %) 1.752 ± 0.551 (70.82 %) 31.36 ± 5.90 (1.51 %) 46.38 ± 2.26 (0.67 %) χ^2=1.317
0.13 ± 0.01	0.045 ± 0.0005 (0.03 %) 2.372 ± 0.049 (2.11 %) 5.991 ± 0.356 (97.85 %) χ^2=1.072	1.78 ± 0.04	0.164 ± 0.003 (1.45 %) 1.194 ± 0.087 (51.86 %) 2.107 ± 0.166 (46.69 %) χ^2=1.290
0.25 ± 0.01	3.023 ± 0.085 (4.25 %) 5.913 ± 0.347 (95.75 %) χ^2=1.094	2.03 ± 0.05	0.102 ± 0.002 (1.95 %) 1.051 ± 0.028 (35.43 %) 2.024 ± 0.067 (62.62 %) χ^2=1.246
0.51 ± 0.01	0.039 ± 0.0009 (0.54 %) 1.887 ± 0.057 (1.72 %) 5.701 ± 0.587 (97.74 %) χ^2=1.071	2.54 ± 0.06	0.217 ± 0.007 (1.24 %) 1.253 ± 0.200 (57.77 %) 2.159 ± 0.291 (40.99 %) χ^2=1.400
0.76 ± 0.02	0.037 ± 0.0004 (0.38 %) 1.881 ± 0.044 (3.05 %) 5.574 ± 0.288 (96.57 %) χ^2=1.088	3.05 ± 0.07	0.104 ± 0.003 (1.23 %) 1.085 ± 0.113 (36.72 %) 1.916 ± 0.251 (62.06 %) χ^2=1.324
1.02 ± 0.02	0.055 ± 0.001 (0.60 %) 1.868 ± 0.072 (3.24 %) 5.467 ± 0.545 (96.16 %) χ^2=1.099	3.56 ± 0.08	0.164 ± 0.003 (1.45 %) 1.194 ± 0.087 (51.86 %) 2.107 ± 0.166 (46.69 %) χ^2=1.212
1.14 ± 0.04	0.112 ± 0.002 (1.11 %) 1.145 ± 0.027 (3.37 %) 5.311 ± 0.420 (94.40 %) 14.82 ± 0.48 (1.12 %) χ^2=1.092	4.06 ± 0.09	0.151 ± 0.002 (1.46 %) 1.190 ± 0.044 (49.10 %) 2.112 ± 0.083 (49.44 %) χ^2=1.306
1.27 ± 0.03	0.047 ± 0.007 (4.71 %) 0.320 ± 0.047 (7.06 %) 1.056 ± 0.124 (10.45 %) 5.178 ± 0.684 (77.78 %) χ^2=1.109	4.57 ± 0.11	0.179 ± 0.003 (3.02 %) 0.790 ± 0.020 (16.44 %) 1.811 ± 0.076 (76.70 %) 6.586 ± 0.150 (3.84 %) χ^2=1.325

a. Fluorescence lifetime measurements made by TCSPC with a 477 nm excitation and an 8 MHz repetition rate. The raw data is fitted using distribution analysis. The error is the standard deviation of the distribution and the value in brackets is the percent intensity attributed to the given decay component.
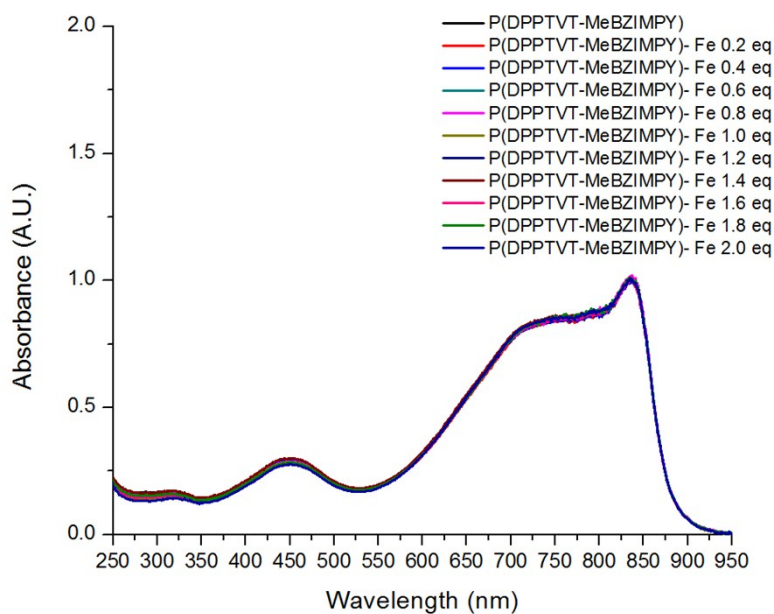
Figure S5. *UV-Visible spectroscopy obtained for P(DPPTVT-MeBZIMPY) upon progressive incorporation of Fe(BF₄)₂.*
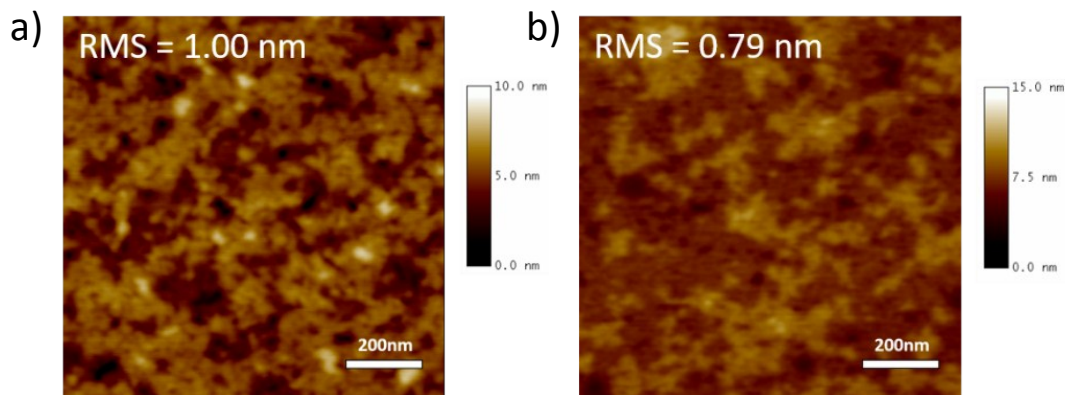

Figure S6. *Atomic force microscopy (AFM) height image of P(DPPTVT-MeBZIMPY) a) before and b) after coordination of Fe(II) ions.*
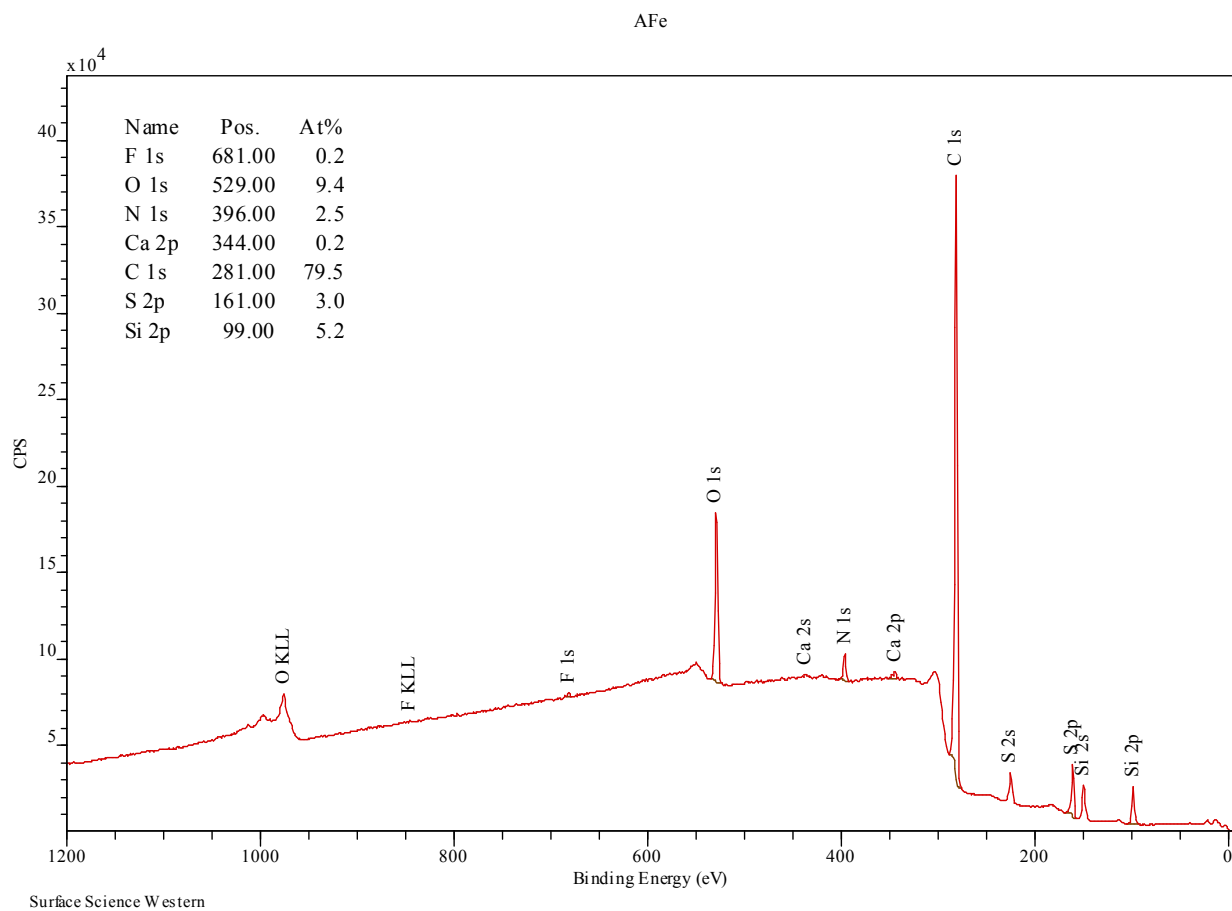
AFe

Name	Pos.	At%
F 1s	681.00	0.2
O 1s	529.00	9.4
N 1s	396.00	2.5
Ca 2p	344.00	0.2
C 1s	281.00	79.5
S 2p	161.00	3.0
Si 2p	99.00	5.2

Surface Science Western

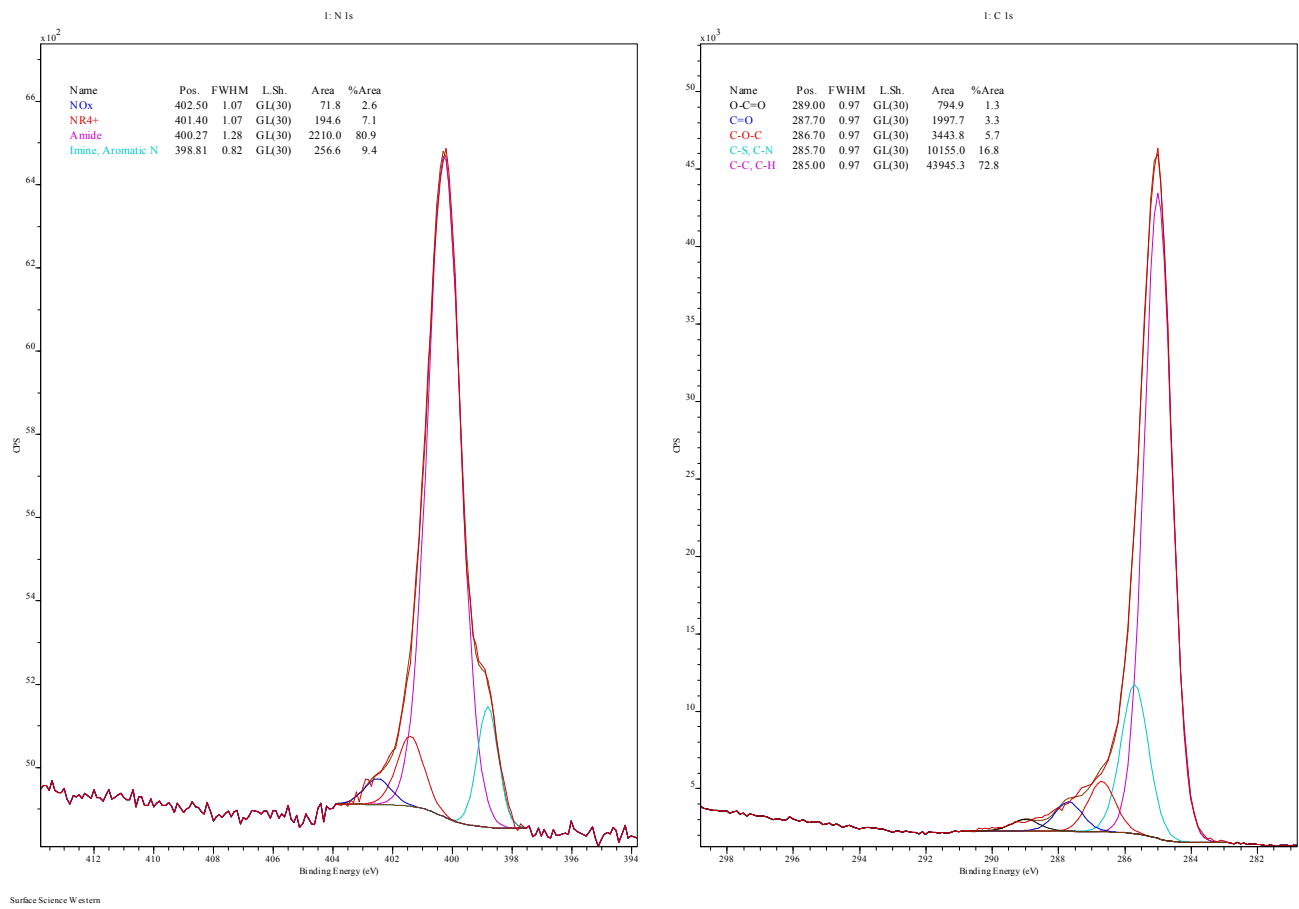**Figure S7.** *X-ray photoelectron spectroscopy (XPS) survey scan of P(DPPTVT-MeBZIMPY)Fe.*

Figure S8. *High resolution X-ray photoelectron spectroscopy (XPS) scans of N 1s and C 1s in P(DPPTVT-MeBZIMPY)-Fe.*

Table S3. *Atomic percentage of P(DPPTVT-MeBZIMPY)-Fe estimated by X-ray photoelectron spectroscopy (XPS).*

Sample Identifier	C	Ca	F	N	O	S	Si
P(DPPTVT-MeBZIMPY)Fe	79.5	0.2	0.2	2.5	9.4	3.0	5.2

Table S4. *Comparison of D-spacing and π-π stacking between both uncomplexed and complexed polymer materials, as calculated by grazing incident X-ray diffraction (GIXRD)*

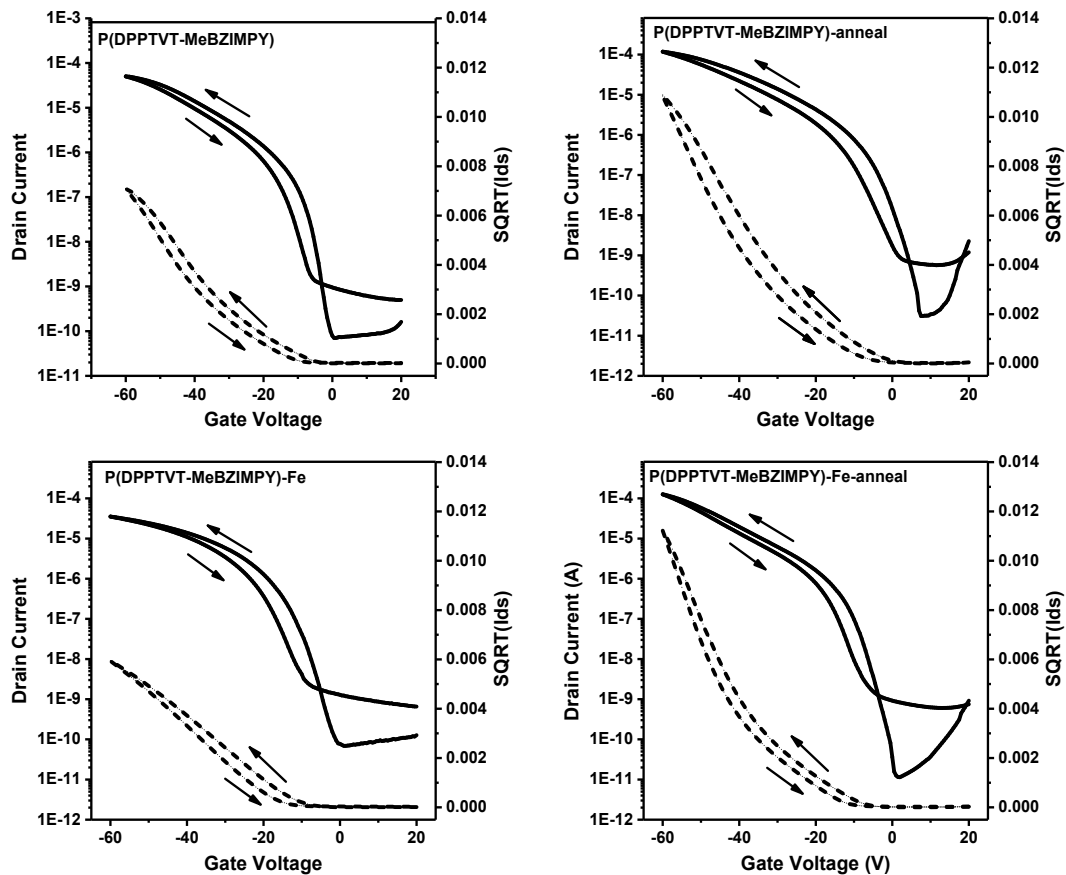| Polymer	D-spacing (Å)	π-π stacking (Å)
P(DPPTVT-MeBZIMPY)	21.6	3.4
P(DPPTVT-MeBZIMPY)-Fe(II)	20.6	3.7

Figure S9. *Transfer curves with hysteresis of OFET devices prepared from P(DPPTVT-MeBZIMPY) and P(DPPTVT-MeBZIMPY)-Fe, before and after thermal annealing at 200°C.*
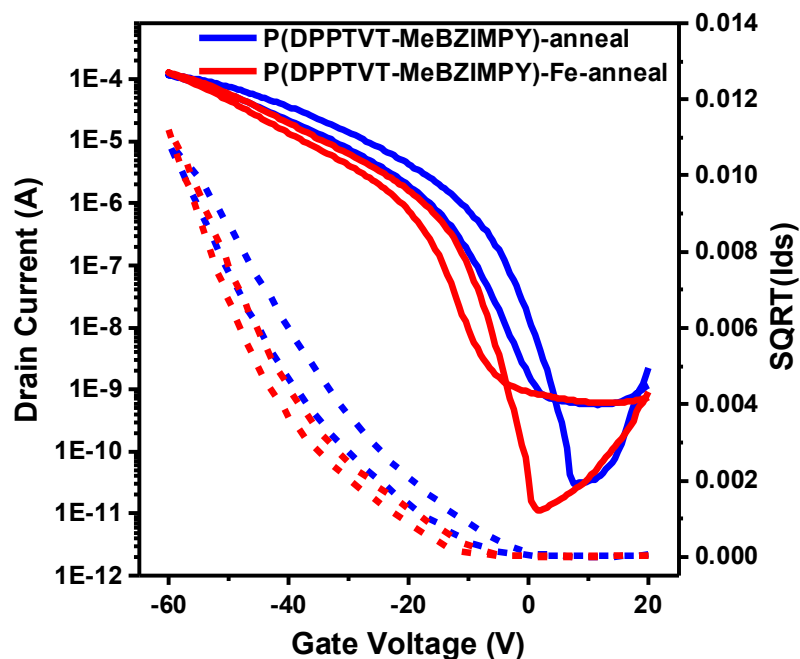
Figure S10. *Transfer curves of organic field-effect transistors prepared from P(DPPTVT-MeBZIMPY) and P(DPPTVT-MeBZIMPY)-Fe, after thermal annealing at 200 ^oC.*
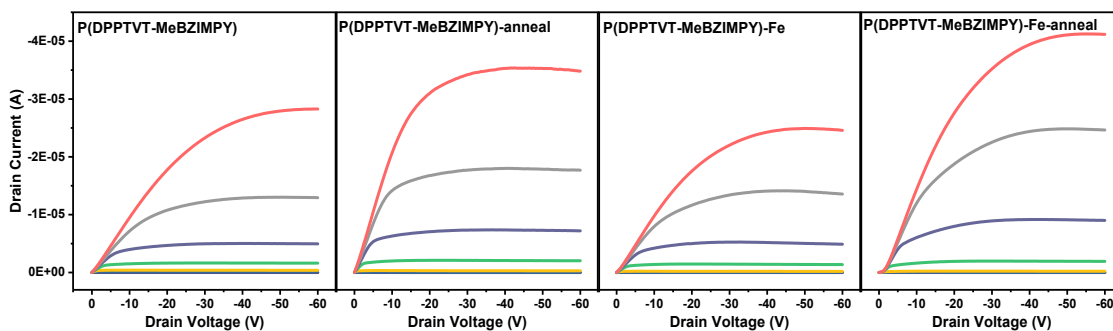

Figure S11. *Output curves (*$I_D - V_D$*) of P(DPPTVT-MeBZIMPY), P(DPPTVT-MeBZIMPY)-Fe, before and after thermal annealing at 200°C. The gate voltage was scanned from 0 to -60V with a step of -10V.*
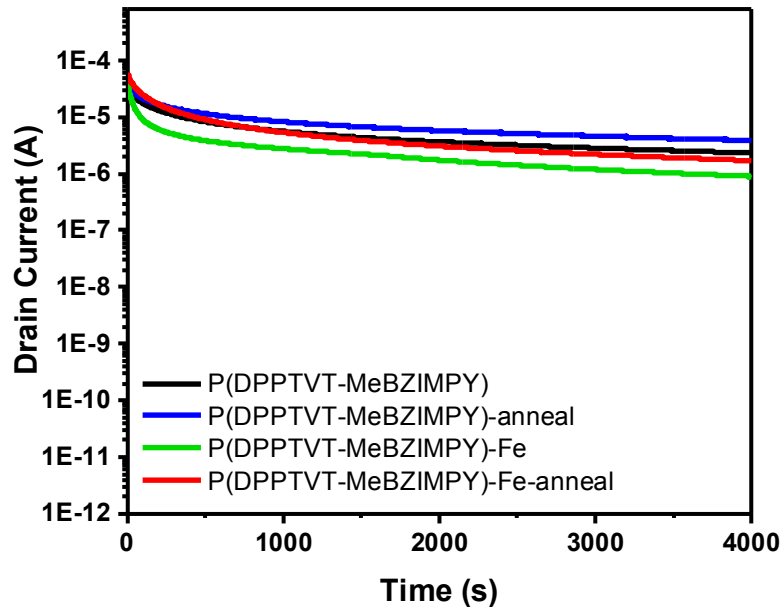
Figure S12. *Retention stability of P(DPPTVT-MeBZIMPY), P(DPPTVT-MeBZIMPY)-Fe, before and after thermal annealing at 200°C·*

References

1   H. Yu, K. H. Park, I. Song, M.-J. Kim, Y.-H. Kim and J. H. Oh. Effect of the alkyl spacer length on the electrical performance of diketopyrrolopyrrole-thiophene vinylene thiophene polymer semiconductors, *J. Mater. Chem. C*, 2015, **3**, 11697–11704.

2   W. Lai, C. Li, J. Zhang, F. Yang, F. J. M. Colberts, B. Guo, Q. M. Wang, M. Li, A. Zhang, R. A. J. Janssen, M. Zhang and W. Li. Diketopyrrolopyrrole-Based Conjugated Polymers with Perylene Bisimide Side Chains for Single-Component Organic Solar Cells, *Chem. Mater.*, 2017, **29**, 7073–7077.

3   F. Pop, J. Humphreys, J. Schwarz, L. Brown, A. Van Den Berg and D. B. Amabilino. Towards more sustainable synthesis of diketopyrrolopyrroles, *New J. Chem.*, 2019, **43**, 5783–5790.

4   Z. Liu, G. Zhang and D. Zhang. Modification of Side Chains of Conjugated Molecules and Polymers for Charge Mobility Enhancement and Sensing Functionality, *Acc. Chem. Res.*, 2018, **51**, 1422–1432.

5   J. Burdyńska, Y. Li, A. V. Aggarwal, S. Höger, S. S. Sheiko and K. Matyjaszewski. Synthesis and arm dissociation in molecular stars with a spoked wheel core and bottlebrush arms, *J. Am. Chem. Soc.*, 2014, **136**, 12762–12770.

6   J. Yao, C. Yu, Z. Liu, H. Luo, Y. Yang, G. Zhang and D. Zhang. Significant Improvement of Semiconducting Performance of the Diketopyrrolopyrrole-Quaterthiophene Conjugated Polymer through Side-Chain Engineering via Hydrogen-Bonding, *J. Am. Chem. Soc.*, 2016, **138**, 173–185.

7   I. Welterlich and B. Tieke. Conjugated polymer with benzimidazolylpyridine ligands in the side chain: Metal ion coordination and coordinative self-assembly into fluorescent ultrathin films, *Macromolecules*, 2011, **44**, 4194–4203.